DOI: 10.21062/mft.2023.059  http://www.journalmt.com

# Exploration of Key Technologies of Intelligent Inspection Robots in the Application of Automatic Energy Meter Verification Line

Xurong Jin (0009-0007-2710-786X)[1], Xinrui Zhang (0009-0000-4722-8350)[1*], Zhiqiang Cheng (0009-0006-4493-4560)[1], Yunpeng Li (0009-0002-5750-6080)[1], Bo Fan (0009-0005-3762-7063)[1], Xu Chen (0009-0009-7484-1500)[1], Xiangwei Wang (0009-0005-6582-2480)[2], Mingqiang Wang(0009-0009-5779-0975)[2]
[1]State Grid Ningxia Marketing Service Center (State Grid Ningxia Metrology Center), China, *e-mail: zhang.b231@yahoo.com
[2] Comarvel Intelligent Technology Company Limited, China

**There are many drawbacks and inconveniences in the application of human power in the energy meter calibration line. In order to achieve a standardized level of operation and to improve the efficiency and quality of the automated meter testing line, this paper applies the intelligent inspection robot to the automated meter testing line and discusses the key technologies involved. Based on the texture characteristics of the screws on the energy meter cover, a screw coordinate positioning method based on the texture center of gravity method is designed as a machine vision technique for intelligent inspection robots. Based on the feedforward controller transfer function and feedback system open-loop transfer function, combined with PI controller, a feedforward-feedback composite servo position control strategy is designed to complete the release action of the robot end controller. Pressure sensor on the robot end claw controller, integrated servo drive with current sensor. The Kalman filter method of static estimation is used to fuse and process multi-source data information to realize the grasping action of the robot end controller. The test results of the key technical performance and economic and time benefits of the robot show that the recognition success rate and grasping success rate of the robot for energy meters are as high as 100%, and it takes a total of 54s to complete each grasping and releasing action. The maximum error in each direction is 4.9mm, 5.2mm and 5.1mm respectively, and the maximum error in angle is only 1.25 degrees. The working manpower is reduced by as much as 93.16%, the average expenditure of inspection cost is only 1.24 yuan, and the floor space is reduced to 700 square meters. In summary, the study can ensure a high level of consistency in the quality of energy meters, improve the efficiency of calibration and production, and create greater economic benefits while providing a solid technical guarantee for the large-scale construction and stable and reliable operation of the power grid.**

**Keywords:** Intelligent inspection robot; Automatic calibration line for energy meters; Machine vision technology; Servo control technology; Torque control technology

## 1 Introduction

As an important electric power measuring apparatus in a large country and a small family, energy meters are related to the national livelihood of thousands of households [1, 2]. Electricity supply enterprises should complete the trade settlement of electricity consumption according to the energy meter. In recent years, the old induction type energy meters are gradually replaced by new electronic type energy meters, and the calibration technology should be constantly innovated [3-6]. The traditional verification and inspection methods are usually done by the staff responsible for the verification and inspection tasks through the program-controlled verification and inspection devices, first hanging the meter on the verification equipment and then disassembling it manually. With the rapid development of market economy and the innovation and reform of electric power system, the speed of smart grid construction has been accelerated, and the goal of regional dressing task of electric energy meter is full coverage, full collection and full fee control [7-9]. The manual work will not only reduce the verification efficiency and operation level, but also cannot meet the increasing demand of energy meters, and make the already heavy daily verification line of energy meters more difficult, and the hidden contradictory problems are more and more obvious and increasing, and the quality also starts to be uneven. Relying on the rapid development of automation technology, the assembly line inspection mode of energy meter automation realizes the automation and intelligent control of all aspects of energy meters from unpacking, out of storage to sealing and labeling by replacing manual with automatic control technology [10-14]. However, according to the new technical specifications of electricity meters introduced by the State Grid

Corporation, the power market has put forward higher requirements for the automated assembly line verification mode of energy meters [15-16]. At the same time, the significant intensification of labor costs has prompted the reform of the inspection mode as an important part of the comprehensive coverage of smart grids in the context of the new era [17].

The level of science and technology continues to escalate, and robots and their extensions, which integrate many technologies such as computers and sensors, have emerged and grown rapidly, and have now become one of the excellent manual replacement technologies for performing work content such as navigation and photography. This represents the comprehensive technological strength of a country, but also means that medical, military, financial and other important areas have the technical support to reach new heights of comprehensive level. The applications of robots in various industries are mostly industrial, agricultural, and medical, for example, the literature [18] designed a jump motion controller with industrial robots as the motion reference. When performing exercises for wrist rehabilitation exercises, the feasibility of the device for assessing and customizing rehabilitation therapy is examined by comparing the measurements of the jump motion controller. The literature [19] used data analysis tools to analyze the results of questionnaires from nearly 1,000 respondents in several countries. It was later found that people's attitude toward the epidemic determined the perception of robot use, and that the panic caused by New Crown pneumonia increased people's trust in and willingness to use service robots. This is because service robots can reduce human-to-human physical contact and narrow the spread of New Crown pneumonia. In the literature [20], in order to discover the dynamic multi-axial loading conditions in the humerus of an amputee population, the humeral kinematics of the population during advanced activities were replicated robotically and humeral trajectories were generated. This research lays the theoretical foundation for the creation of a library of motions that can be used for robotic replication, and the characterization of interactions between prosthesis and bone, giving robots the ability to replicate human motion. In the literature [21], a hybrid best-worst and average-solution distance-based approach is designed to rationally select a robot for a specific application scenario with respect to the different capability requirements of the robot. After comparing with the multicriteria compromise solution ranking method, it is found that the proposed method is highly usable and robust, and has good stability and reliability. The literature [22] optimizes the control capability of the robot using a graphics board according to the type of language developed for the environment of the industrial robot control program. [36] The modular program not only makes the robot adaptive, but also allows operators who are not familiar with the programming language to quickly complete path adjustments. The literature [23] addresses the problem of dynamic and static obstacle recognition and detection for autonomous lawn mowing robots and employs RGB-D cameras to break the limitations of mapping, path planning, and navigation algorithms so that the working area and obstacles can be identified at the same time. Obstacle detection accuracy shows some degree of distortion in the depth data processing pipeline. To improve crop productivity and increase agricultural yields, outdoor agricultural robots and plant phenotyping robots were designed in the literature [24, 25], respectively. The former is based on long and short term memory technology that allows for correct prediction of crop watering times based on current environmental and weather forecasts. By controlling the power and water resources, it ensures that the crops are grown in a suitable enough environment. The latter is mainly used to collect changes in plant morphology as well as chemical and physiological characteristics during time evolution in order to prevent plant trait monitoring errors and provide breeders with valid phenotypic information. The above-mentioned robots and their various technologies have achieved good results. However, there are many types of robots and a wide range of applications, so research should be conducted separately.

The quality is not guaranteed and the cost is getting bigger and bigger with the manual assembly line verification mode of energy meters. As a representative of automation and intelligence, it is urgent to add it to the assembly line inspection mode. To this end, the article takes the intelligent inspection robot as an example and explores the key technologies in its application in the automated energy meter inspection line. First, observe the image of the energy meter captured by the front camera of the intelligent inspection robot, and roughly analyze the meter cover screw texture. The difference image obtained from the first-order differential gradient calculation is used to obtain the screw texture features on the cover of the energy meter. Find the integral image that satisfies the condition and correct the texture information near the screws in the mean binarized image. Based on the statistical characteristics of the screw center cross area obtained from the morphological opening and closing operation, we obtain the center coordinates of the screw and complete the machine vision technique based on the texture center of gravity method for the screw coordinate positioning method. Design feed-forward-feedback composite servo position control strategy to complete the release action of the robot end controller through servo position control. By integrating two devices, a servo driver and a current sensor, the Kalman filter method of static estimation is applied to fuse and process the data information collected by multiple sensors to realize the grasping action at the end of the robot. The above technologies ensure that the intelligent inspection robot can improve the informationization and automation level of the energy meter inspection mode, as well as the efficiency of the assembly line, reduce the negative impact of external factors on the inspection work, accelerate the popularization process of intelligent electricity information collection devices and smart grid, and provide advanced technical support for them.

## 2 Materials and Methods

### 2.1 Key technology of intelligent inspection robot in flowline inspection mode

#### 2.1.1 Machine vision technology

The role of machine vision technology is to guarantee that the robot completes the coordinate positioning of the cover screws without damaging the energy meter. Texture is an important feature of an object. Different types of textures exhibit different characteristics of correlation patterns such as grayscale or color distribution [26, 27]. Therefore, this paper designs a screw coordinate positioning method based on the texture characteristics of the screws on the energy meter cover based on the texture center of gravity method as a machine vision technique for the application of intelligent inspection robots in the inspection assembly line.

First, the energy meter images captured by the front camera of the intelligent inspection robot are observed and the cover screw texture is roughly analyzed. [42] After decomposition in Red-Green-Blue space, the two channels are differenced according to the uniqueness of screw metallic color. [28] The difference image obtained from the first-order differential gradient calculation is used to obtain the screw texture features on the energy meter cover. [29] Next, the eight-directional template of the sobel operator (shown in Fig. 1) is applied to correct the screw coordinates. The conditional definition of the sobel operator is the convolution processing of the received image pixels to obtain the gradient value. The thresholding operation newly generated pixel grayscale values and explicit edge information. [33]

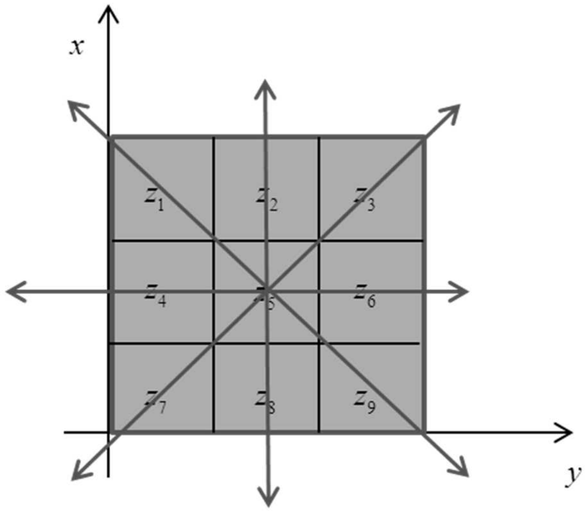


***Fig. 1*** *Schematic diagram of the eight-directional template of the sobel operator*

The energy meter image is processed using eight-directional template filtering to obtain sharpened image grayscale values by the following first-order differential sobel operator.

$$g = \sqrt{S_x^2 + S_y^2} \tag{1}$$

Within this equation, $S_x$ and $S_y$ are the horizontal and vertical filtering templates in the eight-directional template, respectively, and the calculation formula is shown below.

$$S_x = \left[ f(i+1, j-1) + 2f(i+1, j) + f(i+1, j+1) \right] - \left[ f(i-1, j-1) + 2f(i-1, j) + f(i-1, j-1) \right] \tag{2}$$

$$S_y = \left[ f(i-1, j+1) + 2f(i, j+1) + f(i+1, j+1) \right] - \left[ f(i-1, j-1) + 2f(i, j-1) + f(i+1, j-1) \right] \tag{3}$$

According to the obtained texture information, the rectangular area where the screw is located is obtained in combination with the integral image. The upper left corner of the integral image forms a rectangle with one of the coordinate points $(x, y)$, and the value of this coordinate point is the sum of the gray value of each pixel point in this rectangle area. If the localized corner points of this rectangle are $(x_1, y_1)$, $(x_2, y_2)$, and there are $x_2 > x_1$ and $y_2 > y_1$, then the calculation formula is shown as follows.

$$\begin{aligned} &\sum_{x_1 \le x \le x_2} \sum_{y_1 \le y \le y_2} \left[ image(x, y) \right] \\ &= \left[ sum(x_2, y_2) - sum(x_1, y_1) - sum(x_2, y_1 - 1) + sum(x_1 - 1, y_1 - 1) \right] \end{aligned} \tag{4}$$

Explore each pixel row by row and solve the integral map $(I')$. Based on the historical solution value of the integral map, the next integral image value is calculated by adding it to the pixel value $I(x, y)$ of the current initial image $(I)$ in rows.

The equation is shown as follows.

$$I'(x,y)=I(x,y)+I'(x-1,y)+I'(x,y-1)-I'(x-1,y-1) \tag{5}$$

For specific practice, if necessary, extend a column and a row at the leftmost and top of the image. After finding the integral image that satisfies the condition, correct the texture information near the screw in the mean binarized image. If it matches the background texture characteristics near the screw on the cover of the energy meter, the current integral image is the orientation of the screw. The coordinates of the center of the screw are obtained based on the statistical features of the cross area of the screw center obtained by the morphological opening and closing operation [30].

## 2.2 Servo control technology

The inspection robot is able to achieve many tasks such as meter crimping and error checking through grasping and releasing actions, reducing time and cost loss. Among them, the grasping action is realized by servo torque control, and the releasing action is realized by servo position control.

### 2.2.1 Servo position control

The release action of the robot end controller is completed by servo position control. This control method is implemented as follows: When a pulse command is received by the motor driver, the driver compares it with the pulse signal. This pulse signal is obtained from the motor encoder feedback. The deviation is corrected using a position trimmer, and the correction is stopped when the position error is negligibly small. To avoid the tracking delay generated by the traditional PID position controller and to enhance the dynamic response, the feedforward-feedback composite servo position control strategy shown in Fig. 2 is designed.

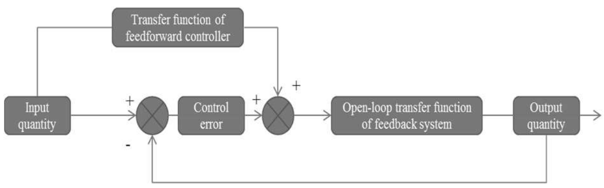


***Fig. 2*** *Schematic diagram of feed-forward-feedback composite servo position control*

The feedforward controller transfer function $F_d(s)$ and the open-loop transfer function $G_c(s)$ of the feedback system are known, and the transfer function definition equation of the feedforward-feedback composite servo position control strategy is derived [31, 32]. As shown below.

$$\Phi(s)=\frac{C(s)}{R(s)}=\frac{G_c(s)\left[1+F_d(s)\right]}{1+G_c(s)} \tag{6}$$

This leads to the transfer function equation for the system deviation shown as follows.

$$\Phi_e(s)=\frac{C(s)}{R(s)}=\frac{1-G_c(s)F_d(s)}{1+G_c(s)} \tag{7}$$

If the feedforward controller transfer function and the feedback system open-loop transfer function satisfy the following inverse equation, the output quantity $C(s)$ is equal to the input quantity $R(s)$ and the control error is 0.

$$F_d(s)=\frac{1}{G_c(s)} \tag{8}$$

The velocity feedforward and acceleration feedforward together constitute the signal feedforward as the position loop of this control strategy, at this time, the expression of the feedforward controller transfer function is shown as follows.

$$F_d(s)=\alpha s+\beta s^2 \tag{9}$$

In this equation, $\alpha$ and $\beta$ represent the velocity gain coefficient and acceleration gain coefficient, respectively [34, 35]. $s$ refers to the independent variable of the transfer function, which can also be called the complex frequency.

The PI controller is used as the original position loop to ensure the positioning accuracy of the servo position control [37]. Combined with the feedforward control strategy, the feedforward-feedback composite servo position control equation for the end of the robot is jointly established. It is shown as follows.

$$Y(K)=k_P E(K)+k_I\sum_{i=1}^{K}E(i)+\alpha\left[R(K)-R(K-1)\right]+\beta\left[R(K)-2R(K-1)+R(K+2)\right] \tag{10}$$

In the above equation, $R(K)$, $R(K-1)$, $R(K+2)$ refer to the value corresponding to the position obtained at the $K$ th, $K-1$ th, $K+2$ th sampling, and $E(K)$ refers to the deviation between this position value and the value corresponding to the feedback position $C(K)$. $k_P$ is the proportional adjustment coefficient of the controller, which plays a fast role in regulating the control error and response speed. $k_I$ is the integral adjustment coefficient of the controller, which plays a role in regulating the steady-state time and residuals.

### 2.2.2 Servo torque control

When the robot executes the grasping action at the end, its claw controller and the energy meter will generate a certain position error, as shown in Fig. 3.

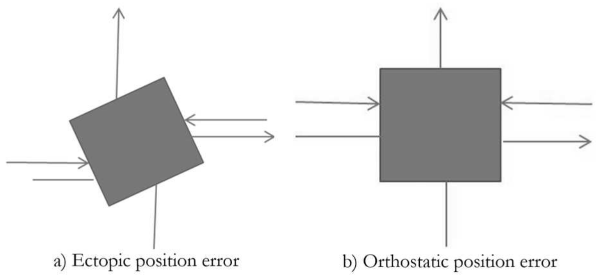


***Fig. 3** Schematic diagram of the position error between the robot claw controller and the energy meter*

In order to obtain good and stable gripping effect, multiple pressure sensors are installed one by one on the end claw controller of the intelligent inspection robot to each claw finger, and the pressure values assumed by different claw fingers are directly fed back. Two devices, servo driver and current sensor, are integrated, and the gripping force condition of the end controller is obtained by multiple sensors. The Atmega 328p tool is used to fuse and process the data from multiple sources of information to obtain accurate and valid information about the force moment. [38-40] Assuming that the armature output current of the servo drive feedback is $I_a$, the equation for calculating the output torque $T_d$ is shown below.

$$T_d = C_T \Phi I_a \tag{11}$$

Within the above equation, $C_T$ refers to the motor constant which is only about the motor structure. $\Phi$ is the air gap flux. According to this equation, a positive correlation between the armature output current and the output torque can be discovered. That is, if the air-gap flux takes a certain value, the output torque increases with the increase of the output current. Therefore, by changing the output current, the torque of the DC motor can be controlled. The Kalman filter method of static estimation is applied to fuse and process the information of data collected by multiple sensors [41]. Based on the measured values of each pressure sensor at time $k$, the converted estimate of the sensor is set to $q_1$ and the converted estimate of the servo drive to the end clamping force is $q_2$. such that the robot end controller does not execute any action command from time $k$ to time $k+1$, and the weighted least square algorithm is invoked to fuse the multi-source information from each sensor [43-44]. The implementation of Eq.

$$s = \sum_{1}^{n} w_i (\hat{q} - q_i)^2 \tag{12}$$

Within this equation, $w_i$ refers to the measurement weight value of the $i$ -time pressure sensor. In order to minimize the multi-source information fusion bias, let the partial derivative of the above equation be zero, and then the following equation is given.

$$\frac{\partial s}{\partial \hat{q}} = 2\sum_{i=1}^{n} w_i (\hat{q} - q_i) = 0 \tag{13}$$

Where:

$$\hat{q} = \frac{\sum_{i=1}^{n} w_i q_i}{\sum_{i=1}^{n} w_i} \tag{14}$$

Assuming that the variance corresponding to the pressure sensor and servo driver commuted estimates are $\sigma_1^2$ and $\sigma_2^2$, respectively, when the weight value and variance satisfy the inverse relationship equation (15), the commuted estimated mean value $\hat{q}$ can be specified in combination with the collected measured values. transforming the above equation into the computational equation (16).

$$w_i = \frac{1}{\sigma_i^2} \tag{15}$$

$$\hat{q} = \frac{\sigma_2^2}{\sigma_1^2 + \sigma_2^2} q_1 + \frac{\sigma_1^2}{\sigma_1^2 + \sigma_2^2} q_2 \tag{16}$$

## 3 Discussion of results

### 3.1 Application of intelligent inspection robots in the automatic energy meter verification line

In order to verify the feasibility of the key technologies of the intelligent inspection robot in the application of the automated meter calibration line, the intelligent inspection robot with these technologies is applied to a running automated meter calibration line. The key technologies of the robot are first analyzed, and then the economic and time benefits of the robot are discussed.

### 3.2 Exploring the technical performance of robotics

The experimental results of the technical performance of different robots were calculated by applying various models of intelligent inspection robots, such as ZWD-qq, FOTRIC 476, ZWD-001, GS300, SA200 and HX-2M, to the automatic energy meter inspection line. The experimental data show that the recognition and grasping success rate of each robot is up to 100%, and each grasping and releasing action takes 54 s. The two sets of data illustrate the effectiveness of machine vision technology and control technology of robots, and the feasibility of robots in the application of automatic meter inspection line. The effective combination of machine vision technology and control technology promotes the successful integration of the intelligent inspection robot with the automatic energy meter inspection line inspection mode. One of the robots is arbitrarily selected, and the end controller running trajectory is fitted with the ideal posture running trajectory as shown in Fig. 4.

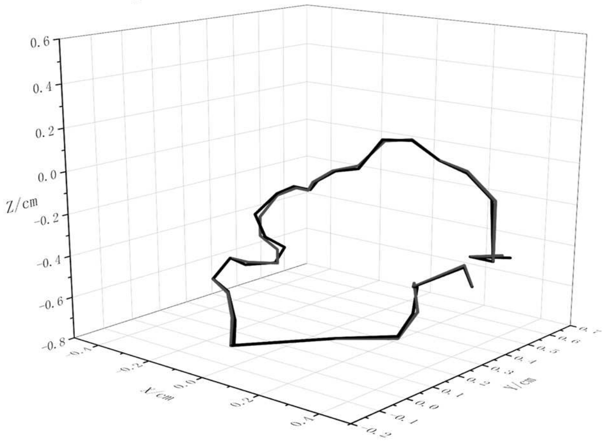


***Fig. 4*** *Schematic diagram of fitting the robot end controller trajectory to the ideal posture trajectory*

From the fitting of the running trajectory of the robot end controller to the ideal pose running trajectory in Fig. 4, it can be seen that by introducing the first-order sobel differential operator in the machine vision technology of the inspection robot, the smoothing processing ability of the random noise contained in the energy meter inspection image is strengthened, and the pixels on both sides of the image edge are enhanced, so that a sharpened image with high contrast and brightness is obtained for the end This provides a reliable reference basis for the accurate operation of the controller. As a result, the feedforward-feedback composite servo-position control strategy and servo-torque control strategy work together to make the trajectory of the robot end controller highly fit to the ideal posture trajectory. The maximum error in the X-direction is only 4.9 mm, the maximum error in the Y-direction is only 5.2 mm, and the maximum error in the Z-direction is only 5.1 mm. The maximum error in the control angle of the end controller is only 1.25 degrees. The position error and angle error are both small, which can meet the operation accuracy of the automatic assembly line verification mode of energy meters.

### 3.3 Exploration of economic benefits

One year after the intelligent inspection robot was put into use on the automated power meter inspection line, as shown in Tab. 1 comparing with the traditional inspection mode; it was found that the work manpower dropped significantly, by as much as 93.16%. The streamlined staff can be expanded to other power supply service teams to optimize the service experience. In the past, the cost expenditure for one inspection of each meter reached RMB 8.98, but now it has been reduced to only RMB 1.24 for each inspection. A total of 5783164 electric energy meters were verified in the experimental cycle. This shows that the application of the intelligent inspection robot has saved the enterprise about 44,867,200 yuan. From the perspective of manpower and controller cost, the use of the intelligent inspection robot has greatly reduced the manpower cost compared with the traditional meter inspection mode. The floor space of the inspection line has also been significantly reduced from 2000 square meters in the traditional manual mode to 700 square meters by virtue of the intelligent and digital advantages of the inspection robot. These data further demonstrate that the designed machine vision technology and servo control technology enable the inspection robot to be used in the automatic meter inspection line in accordance with the requirements of the system.

The machine vision technology and servo control technology allow the inspection robots to accurately complete the meter inspection tasks in the automated meter inspection line, improve the standard and level of the inspection operations, ensure the quality of the meter inspection can be controlled, and enhance the reliability of the meter measurement by accurately and uniformly standardizing the meter values. By adding inspection robots to the automatic meter testing line, the testing capacity can be greatly improved, and the imbalance of meter supply and demand caused by the traditional testing mode can be effectively improved to enhance the efficiency of enterprise turnover. The evolutionary development process from manual mode to robotic inspection mode verifies that the form of electric energy meter inspection is transforming from labor-intensive to technology-intensive, which gives higher promotion value and greater contribution to upgrade and transformation of similar industries, and helps to actively promote the national economic system to resource-saving and eco-friendly forms of development.

***Tab. 1*** *Comparative analysis of economic benefits*

| | **Manual mode** | **Flow line mode** | **Robotic inspection mode** |
|---|---|---|---|
| **Inspection manpower/person** | 3548 | 2432 | 237 |
| **Floor space of flow line/square meters** | 2000 | 1300 | 700 |
| **Assay cost/yuan** | 8.98 | 3.11 | 1.24 |
| **Checking controller cost/yuan** | 0 | 15000 | 8000 |

### 3.4 Time efficiency exploration

This experimental session presents a time efficiency analysis of the application of an intelligent inspection robot in an automated energy meter verification line in two test environments: the laboratory and the verification site. The purpose of the laboratory test is to examine the time efficiency of the meter in the robotic testing mode using a variety of development and commissioning methods. The purpose of the field environment test is to examine the time efficiency of the smart inspection robots in the field by using the assembly line mechanical architecture. The test object starts from the three overall processes of energy meter hanging and line access, calibration process, disassembly and line disassembly respectively. After debugging, it is found that the machine vision technology and servo control technology of the intelligent inspection robot can make the timeliness of the inspection work satisfied, and the application of the robot on the inspection assembly line also strengthens the inspection accuracy of the whole assembly line, so that the robot inspection mode achieves the quality requirements of the energy meter design and factory. The comparative analysis of the time efficiency of the manual mode, the assembly line mode and the robotic testing mode in Tab. 2 shows that the operation of the meter hook-up and line access stage is fully automated, which greatly accelerates the control speed. The time efficiency is reduced from 39.16 minutes in manual mode to 12.87 minutes in line mode and to 2.49 minutes in robotic mode, respectively. In the stage of energy meter verification, the assembly line verification mode with the participation of intelligent inspection robots not only effectively avoids the human verification errors generated by the manual mode, but also improves the verification time efficiency to a certain extent. The time required for calibration has been reduced from 62.44 minutes (i.e. manual mode) to 11.54 minutes (i.e. robotic mode). Similarly, the time efficiency of the meter disassembly and line disassembly stages has also increased significantly. In the traditional manual mode, it takes 32.59 seconds to disassemble a meter and dismantle its wiring. With the application of the intelligent inspection robot to the automated meter calibration line, the time required for the entire meter disassembly and line disassembly is only 7.68 seconds. These test data are sufficient to verify that the intelligent inspection robot with machine vision technology and servo control technology has obvious advantages and broad development prospect in the application of the automatic meter inspection line.

***Tab. 2*** *Comparative analysis of time benefits*

| | **Manual mode** | **Flow line mode** | **Robotic inspection mode** |
|---|---|---|---|
| **Energy meter hookup and line access/minute** | 39.16 | 12.87 | 2.49 |
| **Time required for energy meter calibration/minute** | 62.44 | 23.81 | 11.54 |
| **Energy meter disassembly and wiring disassembly/sec** | 32.59 | 10.15 | 7.68 |

## 4 Conclusion

Energy meter technology is advancing rapidly and the process of building smart grids is accelerating. The project for the replacement of energy meters has been proposed in the strategic guidelines for the construction of the grid, and the full implementation and coverage of energy meters is urgently needed. Although this has a certain development benefit and promotion effect on people's livelihood, it also intensifies the workload of the energy meter verification line and raises the verification requirements. Therefore, in order to meet the increasing demand and quality requirements of energy meters, break the bottleneck of human work efficiency and ensure the quality of energy meter verification, the article explores the key technologies of intelligent inspection robots in the application of automated energy meter verification line. Based on the texture characteristics of the screws on the cover of the energy meter, a screw coordinate positioning method based on the texture center of gravity method is designed and used as a machine vision technique for the application of intelligent inspection robots in the inspection assembly line. The servo torque control technology and servo position control technology are designed to realize the grasping and releasing action for the inspection robot's multiple tasks such as meter level crimping and error checking. After summarizing the practical results of the application of intelligent inspection robots in the automatic energy meter verification line, the following conclusions were obtained.

- (1) Various models of intelligent inspection robots such as ZWD-qq, FOTRIC 476, ZWD-001, GS300, SA200 and HX-2M were applied to the automatic meter inspection line, and the recognition success rate and grasping success rate of each robot were up to 100%, and the total time spent for each grasping and releasing action was 54s. The maximum values of errors in the three axis directions are 4.9, 5.2, and 5.1mm respectively, and the maximum angular error is only 1.25 degrees. The position error and angle error are small, which can meet the operation accuracy of the automatic line verification mode of energy meters and strengthen its reliability and operability as well as informationization and automation level.

- (2) One year after the intelligent inspection robot was put into use on the automatic energy meter verification line, the work manpower dropped significantly, by as much as 93.16%. The cost of one inspection per meter, which amounted to RMB 8.98, has now been reduced to only RMB 1.24 per inspection. The floor space of the inspection line is reduced from 2000 square meters in the traditional manual mode to 700 square meters. These data further demonstrate that the designed machine vision technology and servo control technology can enable the inspection robot to accurately complete the meter inspection tasks according to the instructions on the automated meter inspection line, improve the standard and level of the inspection operation, and provide strong technical support for the future function and performance improvement of the meter inspection line.
- (3) The time efficiency analysis in the two testing environments, laboratory and verification site, shows that the operation time of the meter hook-up and line access phase is reduced from 39.16 minutes in manual mode to 12.87 minutes in assembly line mode, and then to 2.49 minutes in robotic verification mode. The verification phase was reduced from the previous 62.44 minutes (i.e., manual mode) to the current 11.54 minutes (i.e., robotic verification mode). The time for the disassembly and wiring disassembly phase was reduced from 32.59 seconds to 7.68 seconds. These data are sufficient to show that the intelligent inspection robot with machine vision technology and servo control technology can ensure the seamless integration of the automatic meter inspection line work. It not only ensures the reliability of calibration, but also can effectively deal with all kinds of unexpected problems in the process of calibration, which has obvious advantages and broad development prospects.

## References

[1] PENG, L., LI, J., ZHAO, J., et al. (2022). Automatic Verification Flow Shop Scheduling of Electric Energy Meters Based on an Improved Q-Learning Algorithm, *Energies,* Vol. 15. No. 5, pp. 1-11.

[2] SEFERI, Y., BLAIR, S.M., MESTER, C., et al. (2020). Power Quality Measurement and Active Harmonic Power in 25 kV 50 Hz AC Railway Systems, *Energies,* Vol. 13, No. 21, pp. 1-17.

[3] JG, A., DV, B. (2020). Verification of the technical equipment degradation method using a hybrid reinforcement learning trees–artificial neural network system, *Tribology International,* Vol. 153, pp. 106618.

[4] TORRES, E.S., CELEITA, D., SRIRAMULA, S., et al. (2020). Safety Integrity Level Verification Model for IED Protection Schemes, *IEEE Transactions on Industry Applications,* Vol. 56, No. 4, pp. 4329-4336.

[5] SOUREN, T., ROSE, E., GROEPENHOFF, H. (2021). Comparison of Two Metabolic Simulators Used for Gas Exchange Verification in Cardiopulmonary Exercise Test Carts, *Frontiers in physiology,* Vol. 12, pp. 667386.

[6] PERNILLA, L., SOFIA, J., PETRUS, H., et al. (2022). Nasal Lavage Fluid as a Biomedical Sample for Verification of Chlorine Exposure, *Journal of Analytical Toxicology,* Vol. 46, No. 5, pp. 559-566.

[7] ZHAO, Y., DOU, Z., YU, Z., et al. (2022). Study on the Optimal Dispatching Strategy of a Combined Cooling, Heating and Electric Power System Based on Demand Response, *Energies,* Vol. 15, No. 10, pp. 1-18.

[8] BABONNEAU, F., BARRERA, J., TOLEDO, J. (2021). Decarbonizing the Chilean Electric Power System: A Prospective Analysis of Alternative Carbon Emissions Policies, *Energies,* Vol. 14, No. 16, pp. 1-16.

[9] WU, S., DONG, Z. (2022). An Auxiliary Decision-Making System for Electric Power Intelligent Customer Service Based on Hadoop, *Scientific Programming,* Vol. 2022, pp. 1-11.

[10] DÍAZ, S. (2022). Can Shared Control Improve Overtaking Performance? Combining Human and Automation Strengths for a Safer Maneuver, *Sensors,* Vol. 22, No. 23, pp. 9093.

[11] DING, S.Y., LIU, J.L., YUE, M.H. (2021). The Use of ZigBee Wireless Communication Technology in Industrial Automation Control, *Wireless Communications and Mobile Computing,* Vol. 2021, No. 6, 1-11.

[12] MOCANU, D.A., BĂDESCU, V. BUCUR, C., et al. (2020). PLC Automation and Control Strategy in a Stirling Solar Power System, *Energies,* Vol. 13, No. 8, pp. 1-19.

[13] GARANGER, K., KHAMVILAI, T., FERON, E. (2020). Validating Feedback Control to Meet Stiffness Requirements in Additive Manufacturing, *IEEE Transactions on Control Systems Technology,* Vol. 99, pp. 1-8.

[14] NDONDA, G.K., SADRE, R. (2020). Network trace generation for flow-based IDS evaluation in control and automation systems, *International Journal of Critical Infrastructure Protection,* Vol. 31, No. 3, pp. 100385.

[15] SINGH, S., FOZDAR, M., MALIK, H., et al. (2020). Impacts of Renewable Sources of Energy on Bid Modeling Strategy in an Emerging Electricity Market Using Oppositional Gravitational Search Algorithm, *Energies,* Vol. 14, No. 18, pp. 1-20.

[16] SOLIBAKKE, P.B. (2022). Projecting and Forecasting the Latent Volatility for the Nasdaq OMX Nordic/Baltic Financial Electricity Market Applying Stochastic Volatility Market Characteristics, *Energies,* Vol. 15, No. 10, pp. 1-20.

[17] MIHET-POPA, L., SAPONARA, S. (2021). Power Converters, Electric Drives and Energy Storage Systems for Electrified Transportation and Smart Grid, *Energies,* Vol. 14, No. 14, pp. 1-5.

[18] CARBONE, G. (2022). Analysis of the Leap Motion Controller's Performance in Measuring Wrist Rehabilitation Tasks Using an Industrial Robot Arm Reference, *Sensors,* Vol. 22, No. 13, pp. 4880.

[19] MEIDUTE-KAVALIAUSKIENE, I., YLDZ, B., IDEM, E., et al. (2021). The Effect of COVID-19 on Airline Transportation Services: A Study on Service Robot Usage Intention, *Sustainability,* Vol. 13, No. 22, pp. 1-19.

[20] ALIAJ, K., FEENEY, G.M., SUNDARALINGAM, B., et al. (2020). Replicating dynamic humerus motion using an industrial robot, *PLos One,* Vol. 15, No. 11, pp. e0242005.

[21] RASHID, T., ALI, A., CHU, Y.M. (2021). Hybrid BW-EDAS MCDM methodology for optimal industrial robot selection, *PLoS One,* Vol. 16, No. 2, pp. e0246738.

[22] KACZMAREK, W., LOTYS, B., BORYS, S., et al. (2021). Controlling an Industrial Robot Using a Graphic Tablet in Offline and Online Mode, *Sensors,* Vol. 21, No. 7, pp. 1-20.

[23] SKOCZEŃ, M., OCHMAN, M., SPYRA, K., et al. (2021). Obstacle Detection System for Agricultural Mobile Robot Application Using RGB-D Cameras. Sensors, Vol. 21, No. 16, pp. 5292.

[24] WU, C.H., LU, C.Y., ZHAN, J.W., et al. (2020). Using Long Short-Term Memory for Building Outdoor Agricultural Machinery, *Frontiers in Neurorobotics,* Vol. 14, pp. 27.

[25] ATEFI, A., GE, Y., PITLA, S., et al. (2021). Robotic Technologies for High-Throughput Plant Phenotyping: Contemporary Reviews and Future Perspectives, *Frontiers in Plant Science,* Vol. 12, pp. 1082-1082.

[26] MOSHIRI, M., LOALDI, D., ZANINI, F., et al. (2021). Analysis of an as-built metal additively manufactured tool cavity insert performance and advantages for plastic injection moulding, *Journal of Manufacturing Processes,* Vol. 61, No. 5-8, pp. 369-382.

[27] SEPTIARINI, A., SUNYOTO, A., HAMDANI, H., et al. (2021). Machine vision for the maturity classification of oil palm fresh fruit bunches based on color and texture features, *Scientia Horticulturae,* Vol. 286, pp. 110245.

[28] KHATUN, F., AIZU, Y., NISHIDATE, I. (2021). In Vivo Transcutaneous Monitoring of Hemoglobin Derivatives Using a Red-Green-Blue Camera-Based Spectral Imaging Technique, *International Journal of Molecular Sciences,* Vol. 22, No. 4, pp. 1528.

[29] TABASSUM, M.F., AKGÜL, A. AKRAM, S., et al. (2022). Optimal solution of engineering design problems through differential gradient evolution plus algorithm: a hybrid approach,

*Physica Scripta,* Vol. 97, No. 1, pp. 014002-014002.

[30] WANG, T., THOMASSON, J.A., YANG, C., et al. (2020). Automatic Classification of Cotton Root Rot Disease Based on UAV Remote Sensing, *Remote Sensing,* Vol. 12, No. 8, pp. 1310.

[31] WANG, Y., YAO, D., HE, J., et al. (2020). A Stabilization Method Based on an Adaptive Feedforward Controller for the Underactuated Bipedal Walking with Variable Step-Length on Compliant Discontinuous Ground, *Complexity,* Vol. 2020, No. 2, pp. 1-16.

[32] WAN, N., LI, D., HOVAKIMYAN, N. (2020). A Simplified Approach to Analyze Complementary Sensitivity Tradeoffs in Continuous-Time and Discrete-Time Systems, *IEEE Transactions on Automatic Control,* Vol. 65, No. 4, pp. 1697-1703.

[33] MATUŠ, M., BECHNÝ, V., JOCH, R., DRBÚL, M., HOLUBJÁK, J., CZÁN, A., NOVÁK, M. & ŠAJGALÍK, M. 2023. Geometric Accuracy of Components Manufactured by SLS Technology Regarding the Orientation of the Model during 3D Printing. *Manufacturing Technology*, 23, 233-40.

[34] NAGAMINE, G., JEONG, B.G., FERREIRA, T., et al. (2020). Efficient Optical Gain in Spherical Quantum Wells Enabled by Engineering Bi-exciton Interactions, *ACS Photonics,* Vol. 7, No. 8, pp. 2252-2264.

[35] YANG, Y., DONG, Y. (2022). Dynamics of matter-wave solitons in three-component Bose-Einstein condensates with time-modulated interactions and gain or loss effect, *Physica Scripta,* Vol. 97, No. 2, pp. 025201-025201.

[36] CEDZO, M., JOCH, R., TIMKO, P., HOLUBJÁK, J., CZÁNOVÁ, T. & ŠAJGALÍK, M. 2023. Topology Optimization of Gripping Jaws of Industrial Robot. *Manufacturing Technology*, 23, 25-31.

[37] MOSTAFA, S., ZEKRY, A., YOUSSEF, A., et al. (2022). Raspberry Pi Design and Hardware Implementation of Fuzzy-PI Controller for Three-Phase Grid-Connected Inverter Energies, Vol. 15, No. 3, pp. 1-22.

[38] OU, C., LAM, S.K., SUN, D., et al. (2021). SNR-Centric Power Trace Extractors for Side-Channel Attacks, *IEEE Transactions on Computer-Aided Design of Integrated Circuits and Systems,* Vol. 40, No. 4, pp. 620-632.

[39] SONG, L., SUN, H., XU, K., SHI, X. & ZHOU, Y. 2022. Path Planning under The Hull bottom of Painting Robot Based on Heuristic Multi-robot Cooperation in Ship Manufacturing. *Manufacturing Technology*, 22, 218-30.

[40] CSERVENÁK, Á. 2021. Path and Trajectory Planning for an Automated Carrier Vehicle Equipped with two Conveyor Belts used in Manufacturing Supply. *Manufacturing Technology*, 21, 164-83.

[41] ZHANG, Y., LI, T., LI, B., et al. (2020). Fault Detection Method of AC Charging Pile in Coastal Cities Based on Kalman Filtering Algorithm, *Journal of Coastal Research,* Vol. 104, No. sp1.

[42] KHEBLI, A., AGUIB, S., NOUREDDINE, C., LALLIA, K. & MOUNIR, M. 2021. Mathematical modeling and numerical simulation of the buckling stability behavior of hybrid beam. *Manufacturing Technology*, 21, 793-804.

[43] KANG, S.Y., KIM, T.H., CHUNG, W.Z. (2020). Hybrid RSS/AOA Localization using Approximated Weighted Least Square in Wireless Sensor Networks, *Sensors (Basel, Switzerland),* Vol. 20, No. 4, pp. 1159.

[44] WERNIK, C. (2020). Extended Multi WLS Method for Lossless Image Coding, *Entropy,* Vol. 22, No. 9, pp. 919.